

Evaluation of thermal conductivity in air permeable concrete for dynamic breathing wall construction

J.M. Wong¹, F.P. Glasser², M.S. Imbabi^{*}

College of Physical Sciences, University of Aberdeen, Kings College, Aberdeen AB24 3FX, Scotland, United Kingdom

Received 22 March 2006; received in revised form 8 April 2007; accepted 11 April 2007

Available online 25 April 2007

Abstract

Air permeable concrete (APC) is potentially useful as a dynamic insulator. The dynamic function is achieved by passing air through the material in the direction of heat flow to facilitate heat recovery. An APC sample of 200 mm length with 60% cement filling of large voids (between 0.5 and 5 mm), was tested between 5 and 10 Pa differential pressures; permeabilities were 0.28–0.32 m²/Pa h, confirming its suitability as a dynamic insulator. To characterise properties it is necessary to determine the static thermal conductivity, i.e., no air flow. A one-dimensional heat flow model for predicting the effective thermal conductivity (λ_e) of APC is developed using as variables the fractions of voids, aggregate and cement paste comprising the material. Measured values of λ_e were 0.7–1.4 W/m K. A theoretical model predicts and further improves the performance and formulation of APC. The water/cement ratio (w/c) also controls the λ_e . Increasing w/c increases the volume of micropores, adding resistance to heat flow.

© 2007 Elsevier Ltd. All rights reserved.

Keywords: Air permeable concrete; Dynamic insulation; Thermal conductivity; Heat recovery; Energy efficiency

1. Introduction

Dynamic insulation, although a fairly new concept, is attracting attention as a means of reducing energy consumption in building while at the same time, improving indoor air quality. The effective thermal conductivity (λ_e) of air permeable concrete (APC) is an important parameter because, if known, one can predict the dynamic U -value (the heat transfer rate per °C per unit area of building envelope) of a wall made of this material under both steady state and transient conditions when air is drawn through the material [1]. Thus λ_e measurement for APC is an essential precursor in predicting the dynamic U -value.

APC is formed using gap graded mono-size aggregates coated with a precisely specified volume of cement paste

and formed/poured in a mould. Typically the material will be used as blocks or panels, although for test purposes, 100 mm diameter and 200 mm height cylinders were used. After setting the APC is highly porous and the voids remain interconnected allowing permeation. The channels are small enough so that significant air flow only occurs at differential pressures at 5 Pa or higher. The porosity of APC is of two types: the intrinsic porosity of hardened cement paste, usually in the nano- and micro-size range, and the deliberately engineered porosity at the mm scale. To avoid ambiguity, we refer to the engineered coarse porosity as “voids”.

APC is a heterogeneous material consisting of three different material fractions distributed uniformly within the structure: λ_e is the average thermal conductivity of APC as a whole and refers to the case where only heat conduction is taken into account, i.e., no air flow and therefore no heat convection occurs within the internal structure of the material. According to Tavman [2], the effect of heat convection will become significant only if the voids have diameters larger than 1 cm. On the other hand, radiation

^{*} Corresponding author. Tel.: +44 1224 272506; fax: +44 1224 272497.

E-mail addresses: j.wong@abdn.ac.uk (J.M. Wong), f.p.glasser@abdn.ac.uk (F.P. Glasser), m.s.imbabi@abdn.ac.uk (M.S. Imbabi).

¹ Tel.: +44 1224 274480; fax: +44 1224 272497.

² Tel.: +44 1224 272906; fax: +44 1224 272921.

between different interfaces within the material will become important only when temperatures are well above ambient. Since voids diameters in APC in its present development lie in the range between 0.5 and 5 mm and the material operates at or near ambient temperatures, the assumptions that heat radiation and convection are negligible when considering static heat transfer in APC are valid.

2. Literature review of heat flow in multiphase materials

Tavman [2] investigated and summarised a thermal conductivity model for a two-phase material. He compared results from different theoretical models with experimental results on construction sands that varied in porosity. He concluded that no single model could explain and predict the whole range of thermal properties for different porosities; therefore it is necessary to have experimental data. A more recent approach, to determine λ_e by Jagjiwanram [3] considered equivalent thermal resistors formed of two-phases, either in parallel or series arrangement and randomly distributed at an angle θ to the direction of heat flow. The angle θ was calculated from a large number of experiments reviewed in [3]. Since these investigations were limited to two-phase materials this model is not strictly applicable to APC, which is a three-phase material. However Verma et al. [4] reported a λ_e model for a three-phase system using a similar concept of parallel and series slab arrangements distributed at an angle θ . The angle θ was determined as a function of shape of particles, porosity, deviation of heat flux, resistivity formation factor, and the cross sectional area ratio of slabs perpendicular and parallel to the direction of heat flow. The Verma model provides useful insight into the factors that influence λ_e . However it is not practicable, either analytically or experimentally, to determine numerical values for each of these factors and for this reason a different approach is required.

An experimental study by Kim et al. [5] revealed important information on factors affecting the thermal conductivity of conventional concretes. Because the structural formation of APC is different from conventional concrete, empirical results applicable to conventional concrete cannot be applied directly to APC. Nevertheless, some of the material properties developed in [5] for theoretical calculations may be applied.

Existing models able to predict the λ_e of APC are lacking. In order to develop an accurate one-dimensional heat transfer model that is compatible with the temperature boundary conditions that exist in practice, for predicting λ_e in APC and APC-like materials, the following assumptions relevant to static thermal conductivity have been made:

- (i) There is no direct relationship between the angularity and shape of aggregates and λ_e . The shape of aggregate particles mainly affects the packing structure and packing influences the fraction of space available for cement filling. Thus the effect of shape of aggregates

on λ_e can be accounted for as a function of the volume fraction of aggregate filling.

- (ii) The effect of particle size and size distribution is insignificant because λ_e for APC is mainly influenced by the volume fraction of each phase.
- (iii) The change in packing behaviour resulting from interparticle forces between aggregate and cement slurry is assumed to be constant. This assumption is discussed later.
- (iv) The APC is dry, i.e., no bulk liquid water is present apart from exposed surfaces, and the matrix is in equilibrium with the surrounding environment. Thus phase change effects of evaporation or condensation do not affect thermal performance. This is consistent with the use of APC as a dynamic insulation material in a range of climatic environments.

3. Preparation of APC and its measured properties

APC is similar in some respects to 'no-fines' concrete [6,7], the main difference being the greater interconnectivity of voids in APC achieved by manipulating aggregate sizing, cement paste volume and the rheological properties of the fresh mix to obtain the desired permeation. The properties of APC specimens are optimised by:

- (i) Careful control of aggregate sizing by sieving to a narrow selected size fraction.
- (ii) The shape and angularity of aggregates affect how much space is available for cement filling. Shape and angularity will be inferred indirectly from the natural packing density of aggregates. The packing density [8] of an aggregate (PD) is used to indicate how well the solid particles of the aggregate would fill the mould volume, and is defined as:

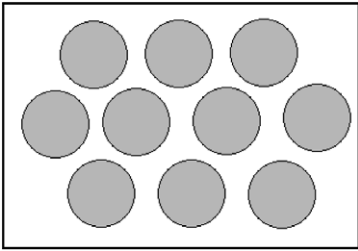

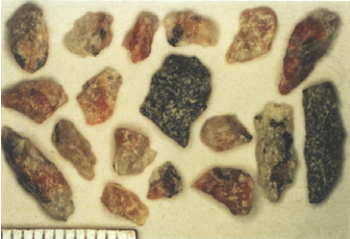
$$PD = \frac{V}{M} \quad (1)$$

where, V is the volume of aggregate and M is the geometric volume of the mould. The natural packing density is defined as the state achieved without compaction or vibration, and is closely related to shape and angularity. Table 1 illustrates these factors.

- (iii) A specified volume of cement paste with other admixtures, determined by the natural packing density of the aggregates used, is mixed with the aggregates before being cast into a mould.

After initial set and demoulding, the APC samples used in laboratory tests were cured underwater for seven days and subsequently allowed to air-dry. When dry, the accessible porosity was measured by the 'Eureka' principle established by Archimedes, using water as the fluid medium with vacuum de-aeration to remove air. Table 2 illustrates the relationship between different type of APC made from irregular-to-slightly rounded aggregate, defined in terms of

Table 1
Shape of aggregate and their packing properties

Shape of aggregate	General description	Natural porosity	Natural packing density*
	<ul style="list-style-type: none"> • Sphere • Perfectly rounded 	0.39–0.40	0.6–0.61
 Scale: 1mm/division	<ul style="list-style-type: none"> • Irregular • Slightly rounded or sub angular 	0.45–0.47	0.53–0.55
 Scale: 1mm/division	<ul style="list-style-type: none"> • Flaky • Highly angular • Elongated 	0.50–0.51	0.49–0.50

w/c and degree of filling (DF), and the resulting physical properties of crushing strength, permeability and porosity. DF is essentially the volumetric ratio of the fresh cement matrix to that of the interconnected voids formed by the intrinsic packing properties of the aggregate, which is in turn affected by their shape and angularity. The natural packing densities for different aggregates were determined in a cylindrical mould 100 mm diameter and 200 mm high. It is expected that packing may vary with the provenance of the aggregate, so the values obtained are not necessarily generic. Edge effects are considered to cancel out when comparing measurements for different aggregates having the same size distribution and the same mould is used in sample preparation. The numerical values of the properties are averages from repeat multiple tests. The strength of APC is sensitive to changes in w/c ; permeability and porosity are less affected by w/c but are strongly influenced by the DF.

The volume fraction of each phase for a dry concrete specimen, i.e., void, cement paste and aggregate, can be determined using Eqs. (2)–(4).

$$\phi_c = (D \times P) - C \quad (2)$$

$$\phi_a = 1 - P \quad (3)$$

$$C = \phi_v + \phi_a + s(D \times P) - 1 \quad (4)$$

Table 2
Measured properties of air permeable concretes (0.53–0.55 natural packing density) with different formulations

Water/cement weight ratio	Degree of filling	Strength (MPa)	Averaged permeability ($\text{m}^2/\text{Pa h}$)	Averaged concrete porosity
0.25	0.5	10.8	0.60	0.32
0.25	0.6	18.2	0.32	0.28
0.25	0.7	25.0	0.18	0.22
0.30	0.5	10.7	0.60	0.32
0.30	0.6	15.3	0.32	0.28
0.30	0.7	21.0	0.18	0.22
0.35	0.5	8.5	0.60	0.32
0.35	0.6	12.7	0.32	0.28
0.35	0.7	15.1	0.18	0.22

where ϕ_c is the fraction of cement paste, ϕ_a is the fraction of aggregate, ϕ_v the fraction of voids (determined experimentally by measuring the concrete coarse porosity by the Archimedes method), P the voidage of the aggregate without cement, D is degree of filling of concrete specimens and C is the shrinkage of cement paste after drying. Cement paste shrinkage results from surface tension forces, evaporation of free water and the intrinsic shrinkage of the paste.

4. One-dimensional heat transfer model for three-phase materials

The thermal conductivity of APC is related to the volume fraction of its components, i.e., aggregates, cement matrix and the medium (normally air) that fills the inter-connected voids. The high proportion and relatively large size of these voids relative to the micropores within the cement matrix support the assumption that micropores in the cement matrix have a minor impact on heat transfer. Like other heterogeneous materials, the thermal conduction properties of APC will be governed by those of its component materials, the volume fraction of each component and the way each component is distributed within the structure. Early models [9] of thermal conductivity used arrays of n components to describe multiphase heat transfer either in series or parallel elements as is shown in Fig. 1.

Mathematical expressions for the average thermal conductivity $\bar{\lambda}$ for the series and parallel approximations are given in Eqs. (5) and (6) respectively, where λ_i ($i = 1, n$) is the thermal conductivity of a component material and ϕ_i is the volume fraction for a particular component.

$$\text{series : } \bar{\lambda} = \phi_1 \lambda_1 + \phi_2 \lambda_2 + \cdots \phi_n \lambda_n \quad (5)$$

$$\text{parallel : } \bar{\lambda} = \frac{\lambda_1 \lambda_2 \cdots \lambda_n}{\phi_1 \lambda_2 \lambda_3 \cdots \lambda_n + \phi_2 \lambda_1 \lambda_3 \cdots \lambda_n + \phi_n \lambda_1 \lambda_2 \cdots \lambda_{n-1}} \quad (6)$$

In the series arrangement the poorest conductor of its component layer dominates the overall heat conduction. However in the case of a parallel arrangement the best conductor dominates the overall heat conduction.

A representative cross sectional view of APC is shown in Fig. 2. The arrangement of constituents is random, giving a structure that is neither parallel nor series. Accurate modelling of heat flow through such a structure is not simple, due to its randomness and irregularity. As a first approximation it is proposed that the heat flow through APC may be idealized into a simple spherical aggregate covered and bridged by a layer of cement paste, as shown in Fig. 3.

With this model, the heat transfer path in 1-D for only a single aggregate particle covered with cement paste and surrounded by air is considered to be a simplified representation of APC. The heat flow can be modelled as shown in Fig. 4 [10], which depicts conduction paths for all the phases, with multiple heat flow pathways corresponding to air-to-cement, air-to-cement-to-aggregate, and air-to-air heat flows. The heat transfer coefficient in 1-D of APC is thus obtained by extension of the single aggregate model to the entire structure.

Fig. 4 shows there are two paths available for heat conduction; one bypasses all solid material and conducts through air while the other route conducts through the solid composite. Since APC is composed mainly of voids

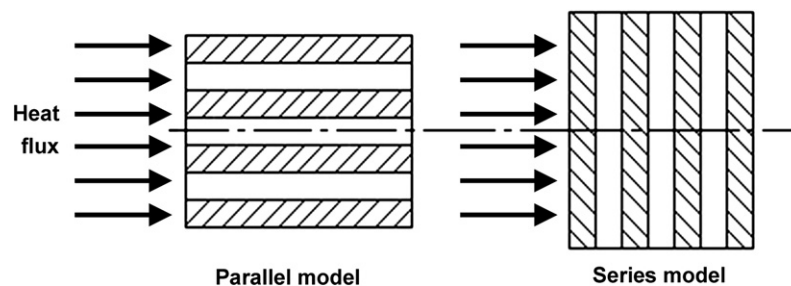


Fig. 1. Multiphase material in parallel and series arrangement.

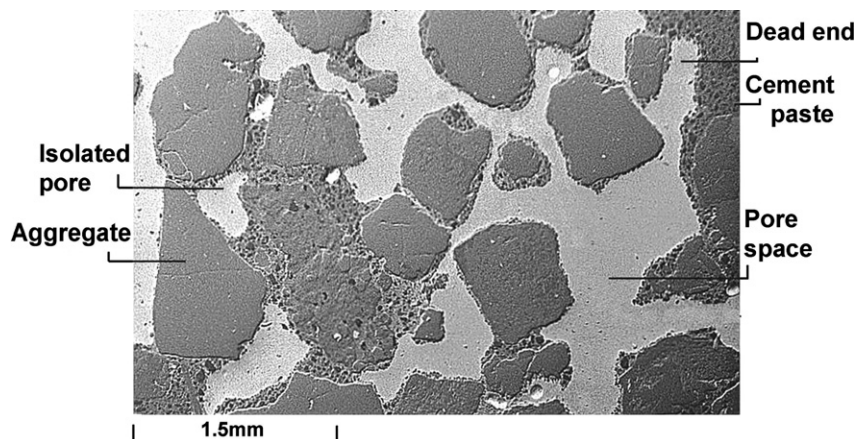


Fig. 2. Cross sectional view of air permeable concrete with 60% degree of filling. The aggregate sieve size is between 0.6 mm (minimum) and 1.18 mm (maximum). The light grey areas are original pores, now resin-filled to permit sectioning.

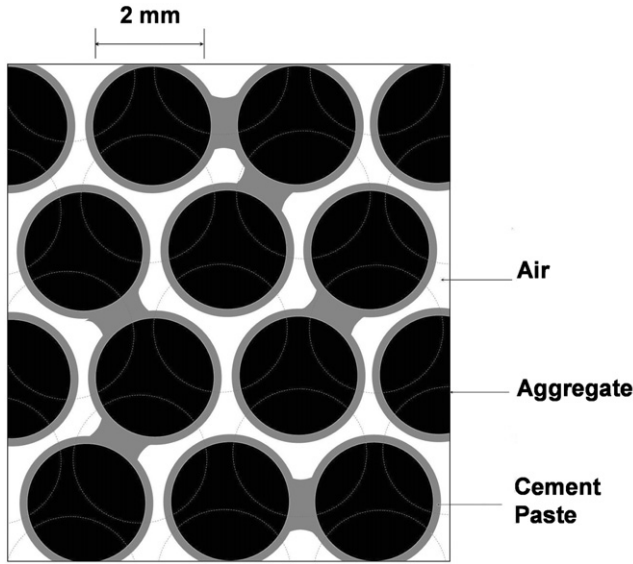


Fig. 3. Idealization of the physical structure of air permeable concrete at the millimetre scale.

and solids and the latter is treated as composite, λ_e can be expressed by Eq. (7).

$$\lambda_e = \phi_v \lambda_v + \phi_s \lambda_{\text{composite}} \quad (7)$$

where ϕ_v is the volume fraction of interconnected voids, λ_v the thermal conductivity of air voids, ϕ_s the volume fraction of solid and $\lambda_{\text{composite}}$ represents the combined thermal conductivity of macro air pockets, aggregate and cement paste. Since air is a poor conductor (0.025 W/m K at standard atmosphere), most of the heat will conduct through the solid composite phase and it is thus reasonable to ignore conduction through air. The solid volume fractions consisting of aggregate (ϕ_a) and cement paste (ϕ_c), give Eq. (8).

$$\phi_s = \phi_a + \phi_c \quad (8)$$

From Eqs. (5) and (6), $\lambda_{\text{composite}}$ can be written as

$$\lambda_{\text{composite}} = \frac{\lambda_v \lambda_c}{\phi_c \lambda_v + \phi_v \lambda_c} + [\phi_c \lambda_c + \phi_a \lambda_a] \quad (9)$$

Substituting Eqs. (8) and (9) into Eq. (7) and assuming that the material is dry, i.e., the voids (interconnected and isolated) are not filled with liquid water, heat transfer will occur mostly by conduction. The resulting expression for λ_e is shown in Eq. (10):

$$\lambda_e = (\phi_a + \phi_c) \left\{ \frac{\lambda_v \lambda_c}{\phi_c \lambda_v + \phi_v \lambda_c} + [\phi_c \lambda_c + \phi_a \lambda_a] \right\} \quad (10)$$

5. Experimental setup and measurement technique

The hot wire method was used to measure thermal conductivity [11–13]. This is a well established, standard technique based on the measurement of temperature rise at a defined distance from a linear heat source embedded in the test material. An idealized model of the hot wire method assumes an infinite thin and long line heat source surrounded by a homogeneous and isotropic material of initial constant temperature. If the heat source has a constant and uniform output along the length of the test specimen, the thermal conductivity can be derived directly from the resulting change in the temperature over a known time interval and the expression for thermal conductivity becomes [2]:

$$k = f \cdot \frac{q \cdot \Delta \ln t}{4\pi \cdot \Delta T} - h \quad (11)$$

where q is a constant quantity of heat production per unit time per unit length of the heating wire and t is the duration of heating in seconds; ΔT is the change of temperature from the initial condition in Kelvins and f and h are specific constants of the measuring probe, whose values were found to be 2.1978 and 0.0626 respectively. The values of f and h were determined by calibrating the measuring probe using two materials of known thermal conductivity. Extruded Teflon and cast Perspex (PMMA polymer) with known thermal conductivities of 0.30 W/m k and 0.20 W/m k, respectively, were used.

The measuring apparatus, similar to that used in [13], and fitted with sheltered, fully calibrated thermocouples, is shown schematically in Fig. 5. Based on this experimental

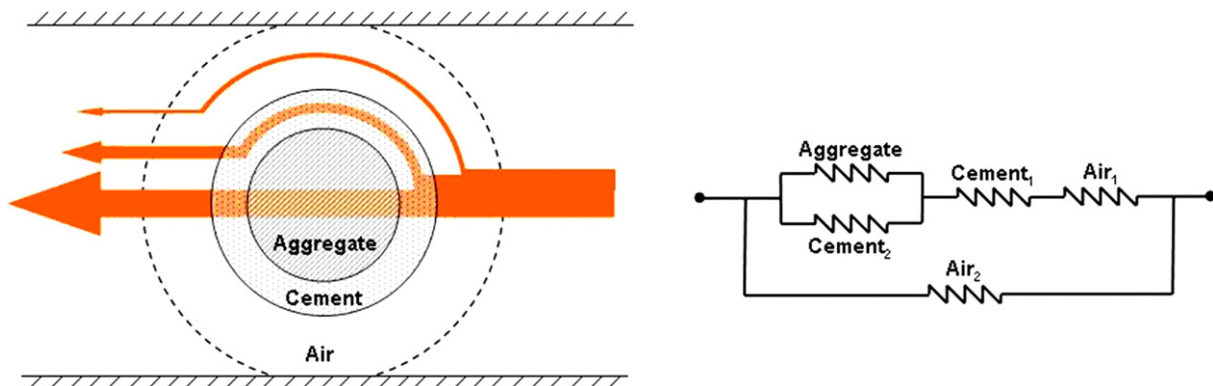


Fig. 4. Material structure (left) and an electrical analogy network model (right) of heat flow in air permeable concrete.

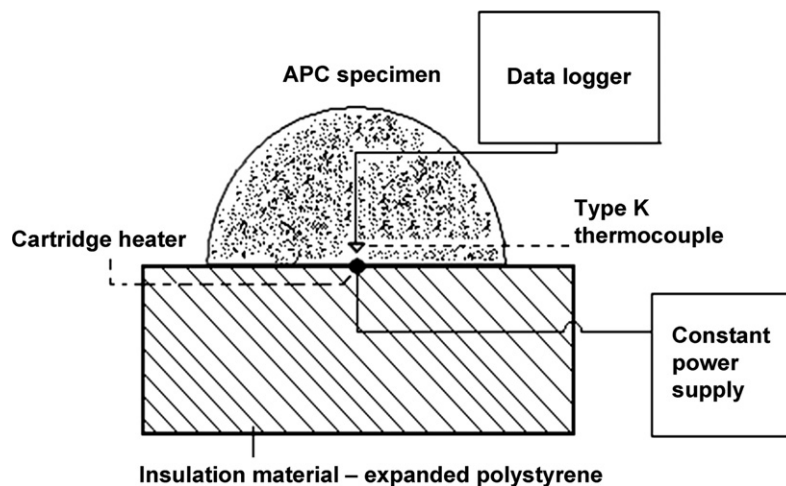


Fig. 5. Schematic of the experimental setup for measurement of static thermal conductivity.

setup Eq. (11) was used to calculate the static thermal conductivity of APC.

5.1. Specimen preparation

The APC specimens tested were made by mixing aggregates of ~ 0.5 natural packing density in combination with different cement formulations. Table 3 summarises the design formulation of the APC specimens and the number of cylinders cast.

The APC specimens were 100 mm in diameter and 100 mm high. After curing for 7 days, each specimen was cut in half lengthwise using a diamond saw giving two identical semicircular cylindrical blocks. By cutting the specimen into two, the potential number of specimens available for thermal conductivity measurements was doubled. Both halves were measured as a test of homogeneity and reproducibility.

5.2. Test procedure

APC samples were placed cut-face on top of a low density expanded polystyrene insulation block. A heater wire positioned beneath the specimen and at the centre-line of a cylinder contacts the surface of the specimen along its entire length. Viewed from one end, the semi-circular

shaped section of the specimen is thus in direct contact with the heater at the centre of the circle. To ensure good thermal contact, a paste (OMEGATHERM[®] 201 Thermal Conducting Paste, supplied by Omega Engineering Inc.) was applied to the contact between heater and specimen. Specimens were shielded to exclude convective and radiant heat transfer effects.

After switching on the heater, the data logger recorded the change in temperature in the specimen at the midpoint with respect to time. This was logged three times at three different currents, each time for a duration of three minutes. Between each log, sufficient time was allowed to permit the specimen to re-equilibrate with the ambient environment. Fig. 6 shows a representative data set. A least squares fit line was plotted between 60 and 180 s of measurement where the rate of change of temperature with respect to time becomes nearly constant in over interval. The slope of the line was then calculated and applied to determine the thermal conductivity of the specimen using Eq. (11).

6. Results and discussion

Table 4 contains the observed data obtained from the experiments. The first two digits of the 'specimen ID', prefixed by a capital D, define the degree of filling of the aggregate voidage. The next two digits represent the water cement ratio by weight, but without the decimal point. The final digit is the reference number of the specimen. For instance, the specimen designated D60/25/1 corresponds to a formulation with 60% void space occupied by cement, a w/c ratio of 0.25, and reference number one. Each concrete specimen was cut into two portions designated as A and B in Table 4. 0.35, 0.45 and 0.60 in Table 4 indicate three different amperages at which measurements took place.

From Table 4, it can be seen that a noticeable increase in λ_c occurs as DF increases. For specimens with the same DF

Table 3
Formulation design and quantity of APC specimens using crushed gneissic granite (natural packing density ~ 0.5)

Degree of filling	w/c	Number of samples tested
0	N/A	1
0.5	0.25	3
0.5	0.35	3
0.6	0.25	3
0.6	0.35	3
1	0.25	3
Total number of specimens		16

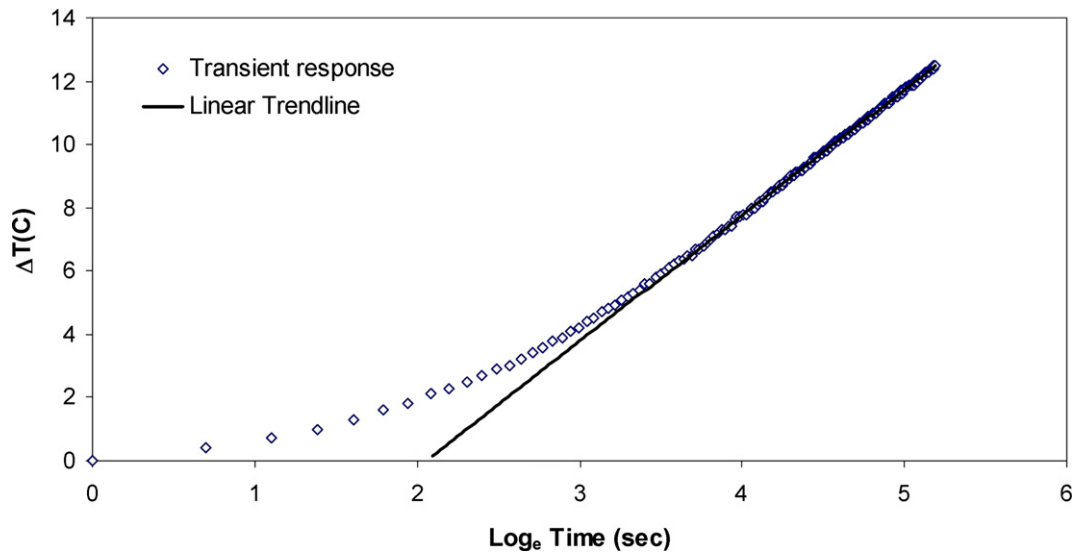


Fig. 6. Experimental temperature rise versus logarithmic time from the experimental setup shown in Fig. 5. A solid line shows the least square fit to the straight-line portion of the curve.

Table 4
Compilation of thermal conductivity measurement of APC using the hot wire method

Specimen ID	Thermal conductivity (W/m K)					
	0.35 A		0.45 A		0.60 A	
	A	B	A	B	A	B
D100/25/1	1.34	1.44	1.34	1.47	1.31	1.40
D100/25/2	1.41	1.53	1.46	1.38	1.47	1.46
D100/25/3	1.50	1.52	1.49	1.45	1.45	1.46
D60/25/1	0.97	1.08	0.97	0.99	0.97	1.00
D60/25/2	1.07	1.00	1.02	1.01	1.06	1.02
D60/25/3	0.96	1.03	1.00	1.01	1.01	0.99
D60/35/1	0.94	0.96	0.95	0.96	0.94	0.95
D60/35/2	0.90	0.92	0.91	0.91	0.9	0.89
D60/35/3	0.89	0.84	0.88	0.89	0.87	0.87
D50/25/1	0.90	0.94	0.89	0.95	0.86	0.94
D50/25/2	0.90	0.87	0.95	0.84	0.92	0.85
D50/25/3	0.95	0.83	0.93	0.85	0.89	0.89
D50/35/1	0.83	0.75	0.81	0.75	0.78	0.73
D50/35/2	0.79	0.74	0.78	0.75	0.81	0.72
D50/35/3	0.66	0.59	0.64	0.62	0.72	0.61
D 0/0/1	0.19	N/A	0.19	N/A	0.20	N/A

an increase in w/c leads to a decrease in λ_e . The values of λ_e in Table 4, are plotted in Fig. 7, to graphically illustrate these trends. The predicted values of λ_e , obtained from Eq. (10), are also shown. Clearly, the experimental results are uniformly lower than predicted values although the trends are similar.

Neither the theoretical curves nor experimental data in Fig. 7 extend down to zero DF. The sharp change observed between the predicted curve and experiment data as the DF approaches zero is thought to be due to surface tension forces arising from the presence of fluid cement, which tend to affect freedom of movement in aggregate packing. As a result, the space-filling differs from that occurring in the

presence of only air–aggregate interfaces [14]. It is shown in [14] that this dramatic change in porosity becomes important at between 0% and 3% of slurry relative to weight of aggregate. As this limit is always exceeded in practical formulations for APC, the natural packing density was used in the calculations. The effect of interparticle force relationships in the presence of cement slurry and its complex interaction with the water evaporation and real intrinsic paste shrinkage within the APC structure are not taken into account in this model but are approximately constant for all practical formulations.

Fig. 7 reflects a similar trend between predicted and measured thermal conductivity, but there are differences. In particular, the calculation over-estimates conductivity and is not sensitive to water: cement ratio (w/c). At the lower water: cement ratio (0.25), essentially all of the water becomes chemically bonded in the hydrated cement and is retained in the gentle drying conditions used. However, at the higher water content ratio of 0.35, excess water evaporates in the course of drying leaving a more porous cement. The micropores developed at higher w/c ratios make the cement a better insulator, albeit at the expense of strength. Since w/c is a important parameter, especially in respect of strength development, another approach was taken; Eq. (12), taken from [15], was used to explicitly introduce a cement porosity factor based on w/c .

$$P_t = \frac{w/c - 0.17H}{0.317 + w/c} \quad (12)$$

Eq. (12) relates the intrinsic porosity (micro and nanoporosity) of hardened cement paste to w/c and degree of hydration (H). Experimental results on thermal conductivity for conventional concrete by Kim [5] revealed that aging of concrete beyond a few days does not have a significant effect on λ_e . This therefore suggests that w/c is the main

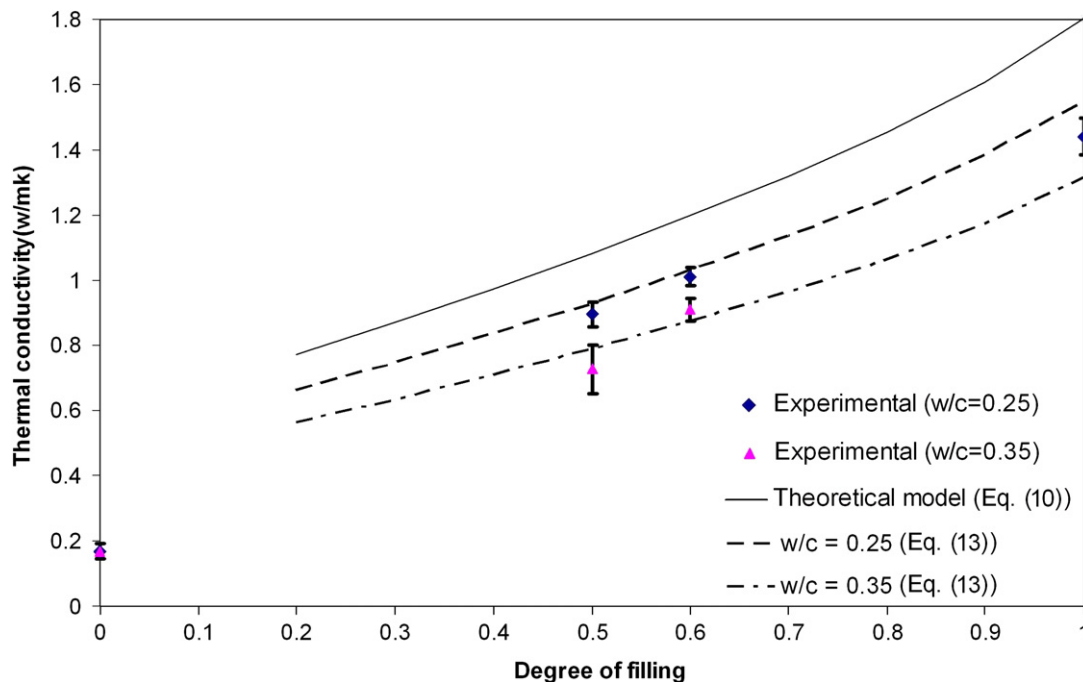


Fig. 7. Experimental and theoretical predictions of effective thermal conductivity λ_e , showing error bars for the measurement.

factor influencing porosity as most concrete/cement product will be well cured, i.e., it will achieve a high degree of hydration before entering service. If the cement is assumed to be fully hydrated and its degree of hydration is equal to 1, the following improved expression for calculating λ_e was developed:

$$\lambda_e = (\phi_a + \phi_c) \left\{ \frac{\lambda_v \lambda_c}{\phi_c \lambda_v + \phi_v \lambda_c} + [\phi_c \lambda_c + \phi_a \lambda_a] \right\} \cdot (1 - p_t) \quad (13)$$

From Eq. (13), λ_e for an APC can thus be predicted as a function of volume fraction of the different components (i.e., aggregate, cement paste and voids), the thermal conductivity of different components and w/c , contained implicitly within the total cement micro/nano porosity (P_t). Fig. 7 confirms that this approach leads to a better fit between the predicted thermal conductivity of APC and its measured value: incorporating the inverse function of porosity clearly offers more reliable predictions.

Even though the predicted results at 0.35 w/c ratio show greater divergence than the measured values at different values of DF, for practical purposes Eq. (13) is accurate enough for overall property prediction, especially when considering the wide variability that can occur in concrete materials. The equation will thus be used in the future to predict performance and assist the design of new higher performance APC materials.

7. Conclusions

An improved analytical model of effective thermal conductivity λ_e for APC has been developed. In order to

validate the analytical model, λ_e was also measured experimentally using the hot wire method. The combination of experimental and analytical data has provided a potent means of further refining the model, enabling a semi-empirical expression for λ_e to be validated. To summarise, the main findings of the study are as follows:

- (i) For APC in thermal equilibrium with the ambient environment and in a dry state the main factors influencing the value of λ_e are the volume fraction of its components, thermal conductive properties of its components and the w/c ratio of the cement paste. Since the volume fraction of aggregate in APC is approximately constant for a particular type of aggregate, the manipulation of volume fraction between air and cement paste is expressed as a degree of filling (DF). Thus, the value of λ_e for APC can be expressed as a function of DF and w/c .
- (ii) A mathematical model has been derived that takes into account the effect of all of the parameters mentioned in (i), including w/c ratio. Predicted results show a good correlation to the experimental data.
- (iii) The model can theoretically be used to predict thermal conductivity for APC specimens with DF range from 0% to 100%. Nevertheless, prediction of APC with less than 50% DF are not supported by experimental result, therefore great caution is needed for predicting the conductivity of low DF APC. Since for the time being APCs with DF lower than 50% do not have sufficient strength for practical application in construction, the model thus fulfills most of the requirements for analysis of static thermal properties of APC.

- (iv) With this model, the effective thermal conductivity of APCs made with aggregates of different mineralogies, e.g., granite or limestone can be predicted. Reduction in the static thermal conductivity of 50% or higher compared to conventional concrete; theoretically much lower dynamic thermal conductivities are possible which would significantly enhance the energy saving potential of APC.
- (v) According to the model that has been developed, APC in the range 50–60% is between 0.78 and 0.85 W/K m for w/c 0.35 and 0.9–1.0 W/K m for w/c 0.25. In comparison, conventional concrete yields values of between 1.4 and 2.0 W/K m depending on mix type. This comparison shows a significant decrease in thermal conductivity due to the increase of voids in the APC structures.

8. Future work

The dynamic thermal conductivity λ_{dynamic} of APC materials is currently being investigated analytically. Early predictions suggest that it will be possible to achieve a dynamic U -value of 2.7 W/K m² (a 30% reduction), when the air flow velocity is 0.002 m/s. Validation of these predictions requires development of a new dynamic U -value test apparatus which is underway. The results will be reported in a subsequent paper. Because of the likely impact of aggregate shape on performance, introducing shape factors into the predictive expressions is thought to be a useful development. Base-line experiments using spherical aggregates are currently in progress to aid our understanding of this factor. This work will be augmented by numerical simulation of the performance of breathable concrete using discrete micro-component models to generate further insights into the mechanical, thermal and filtration properties of the material.

Acknowledgement

This research has been supported by the College of Physical Science at Aberdeen University. Their support is greatly appreciated.

References

- [1] Taylor BJ, Cawthorne DA, Imbabi MS. Analytical investigation of the steady state behaviour of dynamic and diffusive building envelopes. *Build Environ* 1996;31(6):519–25.
- [2] Tavman IH. Effective thermal conductivity of granular porous materials. *Int Commun Heat Mass Transfer* 1996;23(2):169–76.
- [3] Jaggiwanram RS. Effective thermal conductivity of highly porous two-phase system. *Appl Therm Eng* 2004;24(17–18):2727–35.
- [4] Verma LS, Shrotriya AK, Singh R, Chaudhary DR. Prediction and measurement of effective thermal conductivity of three-phase systems. *J Phys D: Appl Phys* 1991;24(9):1515–26.
- [5] Kim K, Jeon S, Kim J, Yang S. An experimental study on thermal conductivity of concrete. *Cement Concrete Res* 2003;33(3):363–71.
- [6] Abadjieva T, Sephiri P. Investigations on some properties of no-Fines concrete. In: Anonymous, editor. 2nd International conference on construction in developing countries. Botswana: CIB; 2000.
- [7] Al-khalaf MN, Yousif HA. Compactibility of no-fines concrete. *Int J Cement Compos Lightweight Concrete* 1986;8(1):45–50.
- [8] Kwan AKH, Mora CF. Effects of various shape parameters on packings of aggregate particles. *Mag Concrete Res* 2001;53(2):91–100.
- [9] Parrott JE, Stuckes AD. Thermal conductivity of solids. London: Pion Ltd; 1975.
- [10] Wong JM, Glasser FP, Imbabi MS. Breathable concrete for low energy building. In: Imbabi MS, Mitchell CP, editors. World renewable energy congress. Aberdeen: Elsevier; 2005.
- [11] Hammerschmidt U, Sabuga W. Transient hot wire (THW) method: uncertainty assessment. *Int J Thermophys* 2000;21(6):1255–78.
- [12] Labudova G, Vozarova V. Uncertainty of the thermal conductivity measurement using the transient hot wire method. *J Therm Anal Calorim* 2002;67(1):257–65.
- [13] Santoyo E, Garcia A, Morales JM. Effective thermal conductivity of Mexican geothermal cementing system in the temperature range from 28 °C to 200 °C. *Appl Therm Eng* 2001;21(17):1799–812.
- [14] Feng CL, Yu AB. Quantification of the relationship between porosity and interparticle forces for the packing of wet uniform spheres. *J Colloid Interface Sci* 2000;231(1):136–42.
- [15] Neville AM, Brooks JJ. Concrete technology. England: Longman Scientific & Technical; 1987.